NUMERICAL SIMULATION OF THREE DIMENSIONAL BOUNDARY LAYER FLOWS

Pier Giorgio SPAZZINI
DIAS, Politecnico di Torino
Torino, Italy

ABSTRACT

A three-dimensional boundary layer computational code is tested on a typical 3D configuration (ellipsoid at incidence).

Output of the program is compared to experimental results and to results obtained by a less sophisticated code.

A significant improvement is observed with respect to the former code; results show a qualitative good fit to experimental data, but quantitative values are still to be improved.

INTRODUCTION

Numerical simulation is becoming a more and more important tool in the Fluid Dynamics field as the experimental costs increase and the numerical ones decrease.

Experimental costs are increasing because:

- The growing requests the designer must face impose the study of quantities of configurations, and inside each of them a parametric study. The complete experimental study of a project would then require an incredible amount of wind tunnel runs.
- Meanwhile, the operating costs of the wind tunnel themselves are rapidly increasing because the needs, mentioned above, for always better precision, call for higher and higher flow quality in the test section, which in turn leads to higher wind tunnel costs.

The numerical costs are on the other hand decreasing as the computer design evolution allows the production of machines which have always higher performances and better cost-effectiveness.

Anyway, a full simulation of the flow is still beyond the possibilities of the existing technology (except for some particular cases, namely low Reynolds number flows); then, the flow must be modeled or simplified in some way for its numerical study.

These simplifications and modeling need to be carefully evaluated by checking the numerical results against experimental data in at least some test cases (validation of the code). The tests used for the validation should be as close as possible to the true cases for which computations will actually be made.

A variety of ways have been proposed and developed for the afore mentioned simplification of the flows for the purpose of numerical simulation; one of the ways of modeling a three dimensional boundary layer - which is the one of interest in this work - consists of exploiting the integral equations of the boundary layer (see next section).

This approximation is known to give satisfactory results in the case of two-dimensional flows.

As it will be shown in the present work, also 3D flows can be well computed by such a method. It shuld be mentioned however that integral boundary layer equations can give only the global quantities describing a boundary layer, but they bring no informations about the details of the flow field.

Then, depending on whether or not we are interested in knowing these details, the choice of the computational method will be made.

As a final remark, observe that the 3D boundary layers are a subject of great interest in modern aeronautics as three dimensional effects are getting more and more important in the present research effort to reduce the aircraft drag.

DESCRIPTION OF THE NUMERICAL METHOD

The method implemented in the code validated during this work is an integral method developed by J. Cousteix.

It is based on the integral momentum equations in the longitudinal (streamwise) and transversal (crossflow) directions:

$$\frac{C_{fx}}{2} = \frac{1}{h_1}\frac{\partial \theta_{11}}{\partial x} + \theta_{11}\frac{H+2}{U_e}\frac{\partial U_e}{h_1 \partial x} +$$

$$-K_1\theta_{11} + \frac{\partial \theta_{12}}{h_2 \partial z} + K_1\theta_{22} \quad (1)$$

$$\frac{C_{fx}}{2}\tan\beta_0 = \frac{1}{h_1}\frac{\partial\theta_{21}}{\partial x} + 2\theta_{21}\left(\frac{1}{U_e}\frac{\partial U_e}{h_1\partial x} - K_1\right) +$$

$$+K_2\theta_{11}(H+1) + \frac{\partial\theta_{22}}{h_2\partial z} + K_2\theta_{22} \quad (2)$$

The system is completed by an entrainment equation:

$$\frac{\partial\delta}{h_1\partial x} - \frac{v_E}{U_e} = \frac{1}{\rho_e U_e}\frac{\partial[\rho_e U_e(\delta-\delta_1^*)]}{h_1\partial x} +$$

$$-K_1(\delta-\delta_1^*) - \frac{\partial\delta_2^*}{h_2\partial z} \quad (3)$$

Which, if the entrainment coefficient is expressed this way:

$$\frac{\partial\delta}{h_1\partial x} - \frac{v_E}{U_e} = P(G)\gamma$$

(where $P(G)$ is a function obtained by the similar solutions method)
becomes:

$$P(G)\gamma = \frac{1}{\rho_e U_e}\frac{\partial[\rho_e U_e(\delta-\delta_1^*)]}{h_1\partial x} +$$

$$-K_1(\delta-\delta_1^*) - \frac{\partial\delta_2^*}{h_2\partial z} \quad (3bis)$$

The meaning of the symbols employed is as follows:

- C_{fx} Skin friction coefficient.
- $\gamma = \sqrt{\frac{C_{fx}}{2}}$
- β_0 Angle between limiting (wall) streamline and x direction (direction of the external streamline).
- θ_{11}, θ_{12}, θ_{21}, θ_{22} Momentum thicknesses.
- δ Boundary layer thickness.
- δ_1^*, δ_2^* Displacement thicknesses.
- H Shape parameter.
- G Clauser shape parameter,
- $K_{1,2}$ Geodesic curvatures along the streamlines and along their normals.
- $h_{1,2}$ Metric coefficients of the curvilinear reference system based on the body surface.

The system is then closed by the following seven equations, again obtained by the similar solutions method:

$$\frac{\delta_1^*}{\delta} = \gamma F_1(G)$$

$$\frac{1}{\gamma} = \frac{1}{k}ln(H\ Re_{\theta_{11}}) + D^*(G)$$

$$\frac{\theta_{11}}{\delta_1^*} = \frac{1}{H} = 1 - G\gamma$$

$$\theta_{21} = \delta_2^* + \theta_{12}$$

$$\frac{\delta_2^*}{\theta_{12}} = \Phi_1\frac{H}{1-H}$$

$$\frac{\theta_{22}\delta_1^*}{\delta_2^{*2}} = \Phi_2\frac{1-H}{H}$$

$$tan\beta_0 = \frac{-\delta_2^*/\delta_1^*}{\frac{\epsilon_1}{F_1}\frac{GH}{H-1} - \epsilon_2}$$

Here, F_1 and D^* are functions obtained by the similar solutions method. Remark also that the quantities Φ_1, Φ_2, ϵ_1, ϵ_2 are not new unknowns, as they are functions of G, $Re_{\theta_{11}}$, $T = -\delta_2^*/K_2\delta^2$.

These functions are again obtained by the similar solutions method.

This method can then be easily extended to the case of compressible flow; indeed, it is sufficient to write the similarity solutions profile in the form

$$F' = \frac{U_e - u}{U_e\overline{\gamma}}$$

in order to have all these profiles represented by an incompressible family. If then we substitute in all the equations of the system $\overline{\gamma}$ in the place of γ we can solve the system in transformed, pseudo-incompressible variables which will then be decodified to the actual value of compressible variables by a suitable set of relations. (see [7] for details).

DESCRIPTION OF THE NUMERICAL CODES EMPLOYED

- **COUSTEIX** : this was the code to be tested. It is a FORTRAN code implementing a space marching 3D boundary layer computational procedure based on the afore described Cousteix method.

  The code implements also the compressibility effects and can be used to compute the features of a generic boundary layer over adiabatic wall for mach numbers up to 4.

  The detection of transition within the boundary layer is made using the empirical criterion formulated by Arnal - Habiballah - Delcourt, which allows to take into account the effect of freestream turbulence. A short explanation of this criterion is now given; consider that the beginning of the transition region depends essentially on the boundary layer stability (Which can be correlated to the momentum thickness Reynolds numbers at the neutral stability point and at the point under examination) and on the disturbance amplification, which can be correlated to the flow history. The latter quantity can be expressed by the mean Pohlhausen parameter:

$$\overline{\Lambda_{2T}} = \frac{1}{x_T - x_{cr}} \int_{x_{cr}}^{x_T} \frac{\theta^2}{\nu} \frac{dU_e}{x} dx$$

The effect of freestream turbulence, as said, can also be put into account; an empirical correlation for these quantities is:

$$Re_{\theta,T} - Re_{\theta,cr} = -206e^{25.7\overline{\Lambda_{2T}}}[\log(16.8\,Tu) - 2.77\overline{\Lambda_{2T}}]$$

of course, it is necessary to compute the value of $Re_{\theta,cr}$; this can be done by suitable empirical formulas both in the case of selfsimilar and nonselfsimilar flows.

The requirements of the Cousteix code are as follows: it needs the body geometry, as described by a generic curvilinear coordinate system attached to the body. Moreover, it needs a set of boundary conditions (velocity module and direction at the edge of the boundary layer in each point) and initial conditions. If the calculation starts from a stagnation point, the code is able to provide itself a computation of initial values by using the similar solution method results; else, it needs a set of integral thicknesses.

- **VSAERO** This program consists of a 3D panel method for inviscid flow and of a 2D Head method based on the external flow streamlines for the computation of the boundary layer. A viscous/inviscid iteration is then performed. It was used for three purposes:

  1. Computation of the boundary conditions for the Cousteix method. This way of doing it was preferred to the other possible choice (using the theoretical formula for inviscid pressure distribution around an ellipsoid) because it allows to already take into account the presence of a boundary layer while computing the potential flow.This boundary layer won't be the "correct" one but the approximation is largely sufficient to the purpose (see fig. 1)
  2. Computation of initial conditions for the Cousteix method. As mentioned, this method needs a set of initial boundary layer thicknesses; these are taken from the boundary layer section of this code. Notice that, as this is done in the nose part of the body, the differences between 2D and 3D boundary layer are still not important so that these values can be trusted.

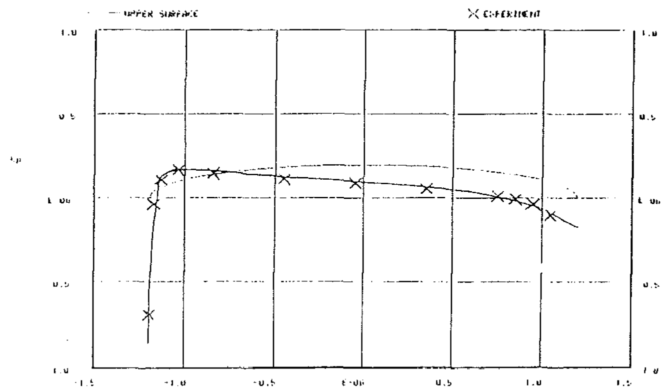

Figure 1: Comparison of C_p distribution along the ellipsoid at $\chi = 37.5^0$; VSAERO (solid line) vs. experimental values (crosses).

  3. Comparison case as less advanced boundary layer solution method.

TEST CASE

The flow over ellipsoids at incidence was choosen as a testcase because of the many advantages it offers:

- It is a highly 3D flow, and includes all the phenomena typical of this kind of flows.
- It is easy to build a mathematical model for it.
- It exists a wide body of experimental results about it.

Two experimental data groups were employed, from DFVLR and from Politecnico di Torino/Chinese Aerodynamical Institute. Both these data blocks were referred to 6:1 ellipsoids (see fig. 2), but absolute dimensions were different; so were the test velocities, resulting in different test Reynolds numbers.

The experimental conditions are resumed in the following table:

Testcase	V (m/s)	a (m)	α (deg)
Göttingen	55	1.2	10
Politecnico	30	0.75	14

In these cases, the transition was imposed by a strip at 20% of the ellipsoid chord.

The transition studies were conducted on the Göttingen ellipsoid. The experimental results were obtained in the various DFVLR wind tunnels, allowing different levels of freestream turbulence.

RESULTS

At first, some different systems of reference were tested over the ellipsoid; this allowed to observe that

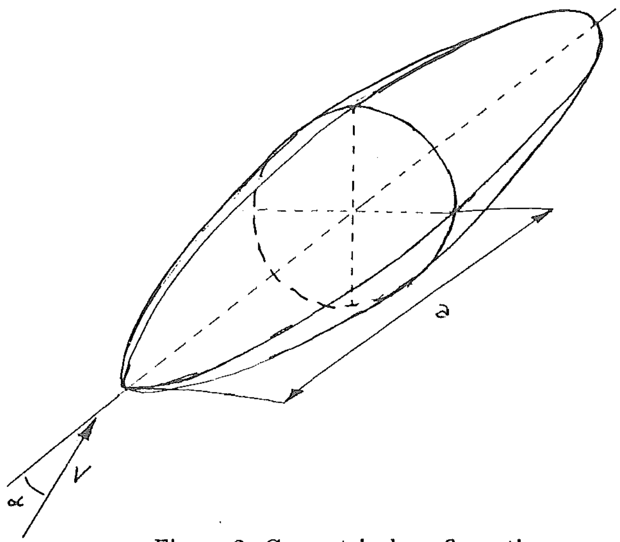

Figure 2: Geometrical configuration

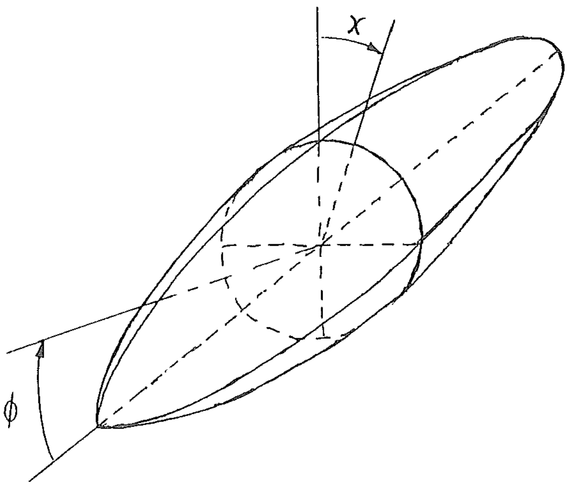

Figure 3: Reference system employed for the Cousteix computations.

the Cousteix code is quite sensitive to the reference system employed; after these tries, the system represented in fig. 3 was choosen.

Consider at first the 3D C_f mapping of figures 4,5.

Observe that the wind side mapping is not very different in the 2 cases, while in the lee side case important differences arise. The most important of these is the presence of the two lighter strakes ($\Leftrightarrow$ lower C_f) predicted by the Cousteix method on the ellipsoid back. They indicate the presence of the two vortices that are known to develop on the back of a 3D body at incidence. The VSAERO code *does not* detect this.

Now consider the 2D quantitative comparisons of figs. 6 to 11.

It is evident from figs. 6,7 that Cousteix's method is sensitive to a physical phenomenon (increase of C_f after a minimum) that VSAERO do not perceive.

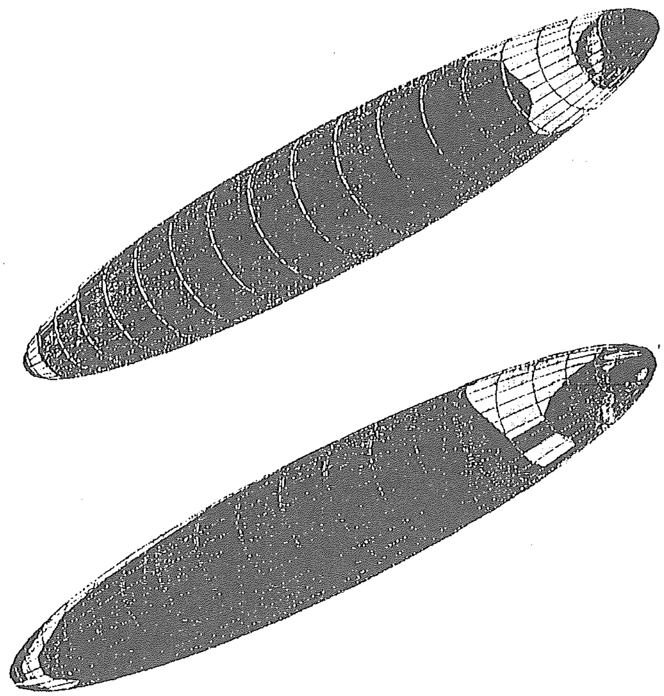

Figure 4: Mapping of the C_f on the wind side of the Politecnico ellipsoid; a) VSAERO, b)Cousteix results.

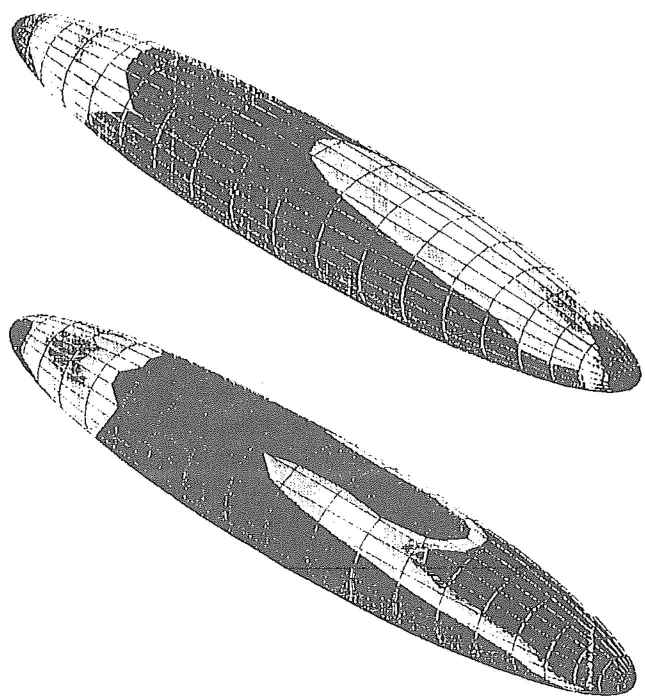

Figure 5: Mapping of the C_f on the lee side of the Politecnico ellipsoid; a) VSAERO, b)Cousteix results.

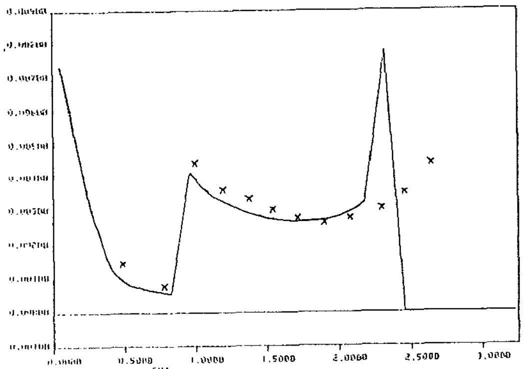

Figure 6: C_f mapping along the ellipsoid, $\chi = 7.5^0$; Cousteix vs. experimental (Göttingen ellipsoid).

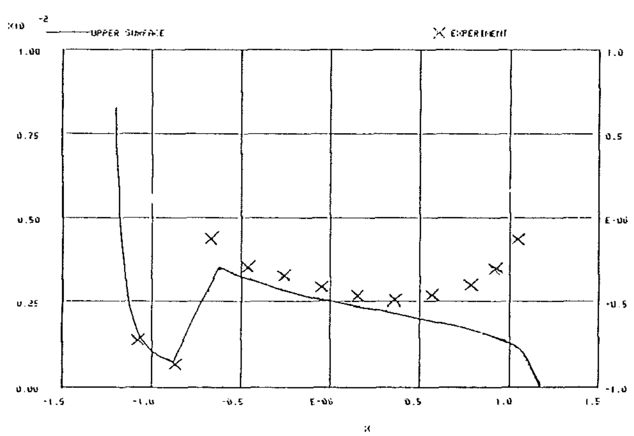

Figure 7: C_f mapping along the ellipsoid, $\chi = 7.5^0$; VSAERO vs. experimental (Göttingen ellipsoid).

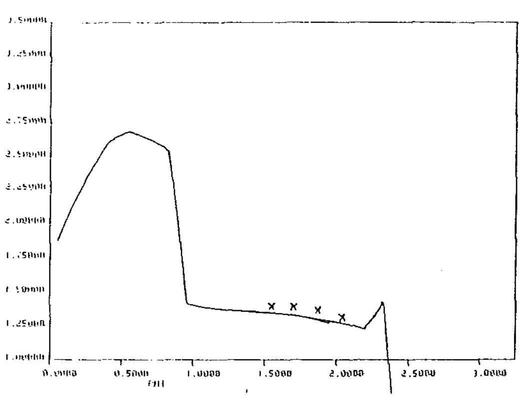

Figure 8: H mapping along the ellipsoid, $\chi = 7.5^0$; Cousteix vs. experimental (Göttingen ellipsoid).

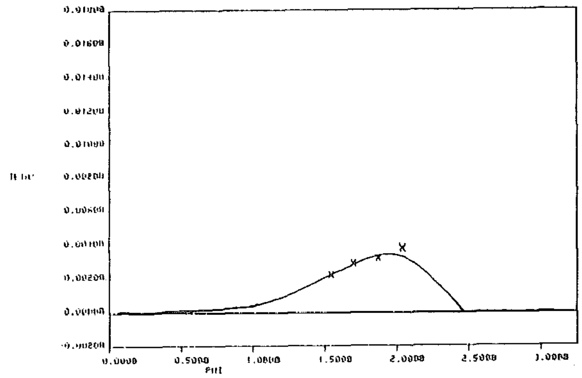

Figure 9: θ_1 mapping along the ellipsoid, $\chi = 7.5^0$; Cousteix vs. experimental (Göttingen ellipsoid).

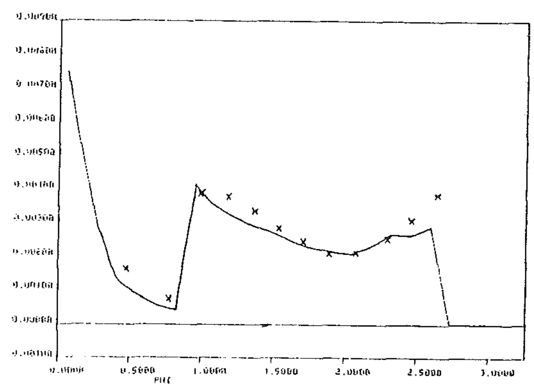

Figure 10: C_f mapping along the ellipsoid, $\chi = 22.5^0$; Cousteix vs. experimental (Göttingen ellipsoid).

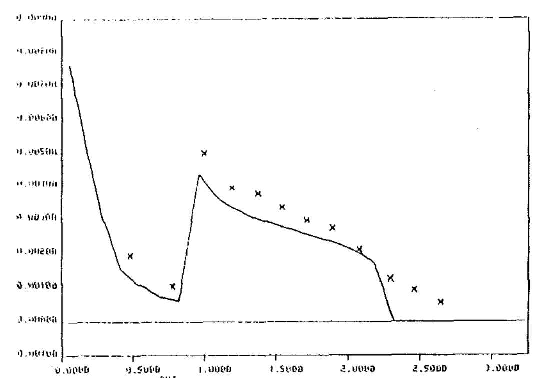

Figure 11: C_f mapping along the ellipsoid, $\chi = 52.5^0$; Cousteix vs. experimental (Göttingen ellipsoid).

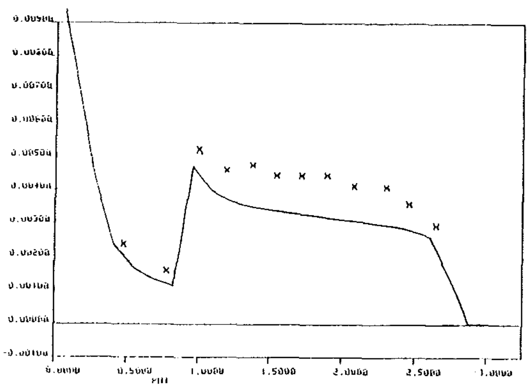

Figure 12: C_f mapping along the ellipsoid, $\chi = 112.5^0$; Cousteix vs. experimental (Göttingen ellipsoid).

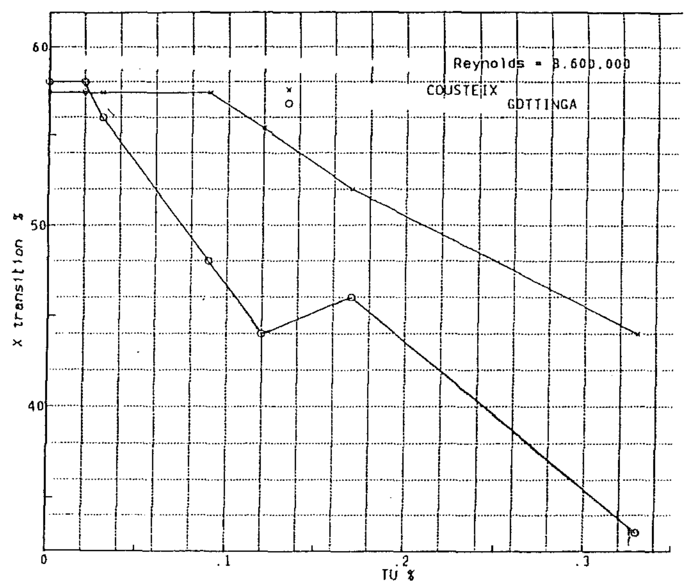

Figure 13: Influence of T_u, freestream turbulence, on the transition point.

Nonetheless, the quantitative analysis of this phenomenon is clearly perfectible. Actually, the program decidely overestimates the extent of the C_f distribution peak.

Distribution of H and θ are well computed.

Going around the ellipsoid, we can observe that Cousteix method indicates the presence of the peak just at the same location as in experimental results. On the lower part, to conclude (fig. 12), we remark that, though the trend is correctly indicated (very flat C_f curve) the program underestimates the values of the skin friction coefficient.

Moving to the analysis of the transition studies (performed only with Cousteix method) it can be observed in fig. 13 that the program gives a good trend for the variation of transition position with variation of T_u, but again the values of the point of transition are

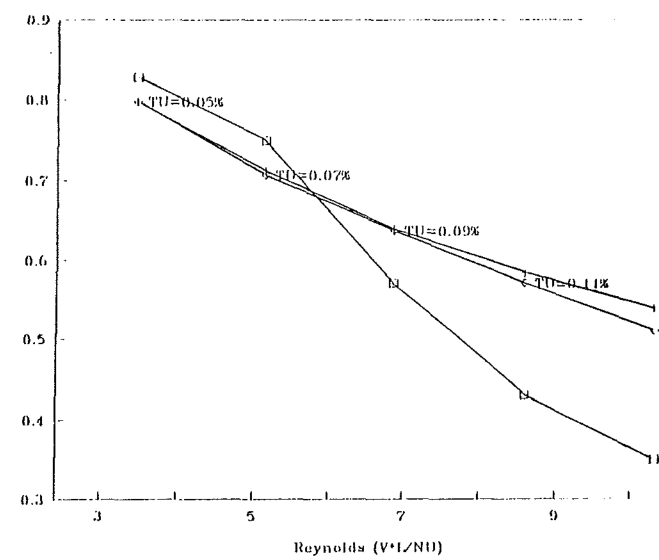

Figure 14: Influence of the freestream Reynolds number on the transition point.

badly computed. The program is able to capture the plateau of transition positions at low turbulence, and it computes quite well its position. The fact that the experimental curve presents a peak can be attributed to the fact that also the turbulence spectrum has an influence on the transition.

Fig. 14 shows the influence of the Reynolds number on transition as predicted by Cousteix method and measured. The two numerical curves were obtained by keeping the T_u constant or linearly varying with airspeed. It can be seen that the difference is not important. Going to the comparison with experiments, again we can observe that the trend is correctly predicted but the values are not very good.

The last parameter considered is the influence of the incidence on the transition; to show this effect, observe fig. 15 (experimental plots) and figs. 16 to 18 : again, the Cousteix method captures the physical phenomena but quantifies them uncorrectly (there is an overestimate of the incidence effect).

CONCLUSIONS

The program tested during this work showed to be satisfactorily reliable.

As described above, it gives good qualitative informations about the flowfield, and quantitative errors are acceptable. Comparison with the VSAERO program allows to state that the new computational procedure is a clear advance in the 3D flowfield computation. Actually, the latter gets some 3D aspects of the flowfield which are out of the VSAERO capabilities, although some imperfections appear in some poins (e.g. the underestimate of the C_f value on the lee side of the ellipsoid).

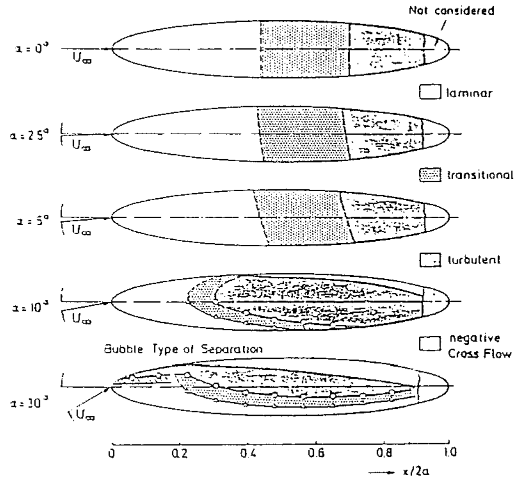

Figure 15: Influence of the incidence on the transition: experimental results.

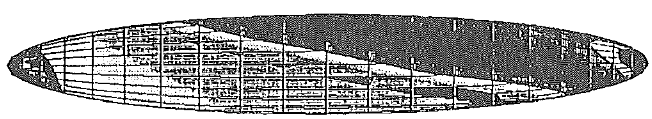

Figure 16: Influence of the incidence on the transition: Cousteix, $\alpha = 5^0$.

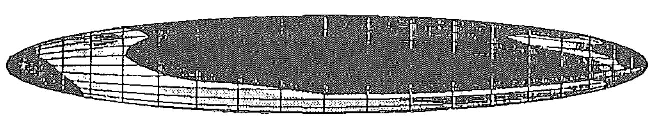

Figure 17: Influence of the incidence on the transition: Cousteix, $\alpha = 10^0$.

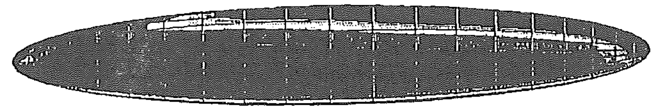

Figure 18: Influence of the incidence on the transition: Cousteix, $\alpha = 30^0$.

Transition is computed with enough precision, and the code showed to be sensitive to many of the parameters that theory and wind tunnel work demonstrated to be important.

Nevertheless, this sensitivity, which under the qualitative viewpoint is good and even very good, is not always supported by a similarly good quantitative agreement. Indeed, the effect of the incidence is often overestimated, while the ones of Reynolds number and external turbulence are underestimated.

ACKNOWLEDGEMENTS

This work was carried on in cooperation with Rinaldo Piaggio Industries.

The author wishes to thank the company for offering the opportunity and providing the facilities to do the work. Thanks go also to the company's technical staff and in particular to engs. Sacco and Casertano and to mr. Sereno.

References

[1] Alim, R. A.: *Three dimensional boundary layer along the lines of simmetry of an ellipsoid* , VKI PR 1986-10, Bruxelles 1986.

[2] Arnal, D.: *Three dimensional boundary layers: laminar-turbulent transition* , AGARD report 741, Bruxelles 1986.

[3] Bradshaw, P.: *Physics and modeling of three dimensional boundary layers* , AGARD report 741, Bruxelles 1986.

[4] Bradshaw, P., Cebeci, T. & Whitelaw, J. H .: *Engineering calculation methods for turbulent flows,* London 1981.

[5] Cebeci, T.: *An approach to practical aerodynamics calculations* , AGARD report 741, Bruxelles 1986.

[6] Clauser, F. H.: *The turbulent boundary layer* , Advances in applied mechanics, Vol. IV, pp. 1-51, New York 1956.

[7] Cousteix, J.: *Analyse théorique et moyens de prévision de la couche limite turbulente tridimensionnelle* , Châtillon 1974.

[8] Cousteix, J.: *Three dimensional boundary layers: introduction to calculation* , AGARD report 741, Bruxelles 1986.

[9] Cousteix, J.: *Cousteix program for 3D boundary layers: program description* , unpublished work.

[10] Hirschel, E. H.: *Evaluation of results of boundary layer calculations with regard to design aerodynamics* , AGARD report 741, Bruxelles 1986.

[11] Iuso, G. & Oggiano, M. S.: *Distribuzione di velocitá in strati limite tridimensionali sviluppantisi su di un ellissoide di rotazione* , unpublished work.

[12] Iuso, G. & Oggiano, M. S.: *Misure di pressione a parete su di un ellissoide di rotazione in incidenza* , unpublished work.

[13] Iuso, G. & Oggiano, M. S.: *Misure sforzo d'attrito a parete su di un ellissoide di rotazione in incidenza* , unpublished work.

[14] Iuso, G., Oggiano, M. S., De Ponte, S., Yuzhong, B. & Xiaodi, Z.: *Boundary layer measurements on an ellipsoid at angle of attack* , Beijing 1987.

[15] Kreplin, H. P., Meier, H. U., Mercker, E. & Landhausser, a.: *Wall shear stress measurements on a prolate spheroid in the DNW Wind Tunnel* , DFVLR report, Göttingen 1986.

[16] Kreplin, H. P., Vollmers, H. & Meier, H. U.: *Wall shear stress measurements on an inclined prolate spheroid in the DFVLR 3m $\times$ 3m Low Speed Wind Tunnel* , DFVLR report, Göttingen 1986.

[17] Maskew, B.: *Program VSAERO: theory document* , Washington 1984.

[18] Meier, H. U. & Cebeci, T.: *Flow characteristics of a body of revolution at incidence* , Long Beach 1985.

[19] Meier, H. U. & Kreplin, H. P.: *Experimental investigation of the boundary layer transition and separation on a body of revolution* , DFVLR report, Göttingen 1980.

[20] Meier, H. U., Kreplin, H. P. & Landhausser, A.: *Wall pressure measurements on a 1:6 prolate spheroid in the DFVLR 3m $\times$ 3m Low Speed Wind Tunnel ($\alpha = 10^0$, $U_\infty = 55m/s$, artificial transition* , DFVLR report, Göttingen 1986.

[21] Meier, H. U., Kreplin, H. P., Landhausser, A. & Baumgarten, D.: *Mean velocity distributions in three-dimensional boundary layers, developing on a 1:6 prolate spheroid with artificial transition ($\alpha = 10^0$, $U_\infty = 55m/s$, cross sections $x_0/2a=$ 0.48, 0.56, 0.64 and 0.73* , DFVLR report, Göttingen 1986.

[22] Meier, H. U., Michel, U. & Kreplin, H. P.: *The influence of wind tunnel turbulence on the boundary layer transition*, DFVLR report, Göttingen 1986.